Experimental evidence of characteristic relations of type-I intermittency in an electronic circuit

Chil-Mim Kim,* Geo-Su Yim, and Yeon Soo Kim
Department of Physics, Pai Chai University, Taejon 302-735, Korea

Jeong-Moog Kim
Laboratory for Quantum Optics, KAERI, Yusunggu, P.O. Box 105, Taejon, 305-600, Korea

H. W. Lee
Department of Physics, Inje University, Kimhae, Kyungnam, 621-749, Korea

(Received 13 May 1997)

We experimentally observe the characteristic relations of type-I intermittency [C.-M. Kim *et al.*, Phys. Rev. Lett. **73**, 525 (1994)] in an inductance-resistance-diode circuit. Near a bifurcation point, the reinjection probability distribution is of the form $x^{-1/2}$, and the characteristic relations are of the form $\langle l \rangle \propto \epsilon^{-1/4}$ and constant when the lower bounds of the reinjection are at and above the tangent point, respectively. The results agree well with theoretical predictions. [S1063-651X(97)01009-X]

PACS number(s): 05.45.+b, 07.50.Ek

I. INTRODUCTION

One of the well-known routes from stable orbits to chaotic state (or vice versa) is intermittency which is characterized by the appearance of intermittent short chaotic bursts between quite long quasiregular (laminar) periods. So far, four kinds of intermittency have been reported; crisis induced intermittency [1], on-off intermittency [2], and one- [3–6] and two-dimensional intermittencies [7]. Among them one-dimensional intermittency is again classifed into four types (types-I, II, III, [3–5], and V [6]) according to the local Poincaré map. Each type has its own characteristic relation. The local Poincaré maps of type-I, -II, and -III intermittencies, as reported by Pomeau and Manneville [3], are $y_{n+1} = y_n + a y_n^2 + \epsilon$ $(a,\epsilon>0)$, $y_{n+1} = (1+\epsilon) y_n + a y_n^3 (a,\epsilon,y_n > 0)$, and $y_{n+1} = -(1+\epsilon) y_n - a y_n^3 (\epsilon,a>0)$, respectively [8]. The characteristic relation of type-I intermittency is $\langle l \rangle \propto \epsilon^{-1/2}$, where $\langle l \rangle$ is average laminar length and ϵ is the channel width between the diagonal and the local Poincaré map. The characteristic relation of type-II and -III intermittencies is $\langle l \rangle \propto \epsilon^{-1}$ where $1+\epsilon$ is the slope of the local Poincaré map [4]. So the importance of the local Poincaré map in the characteristic relations has been well recognized, while the role of the reinjection probability distribution (RPD) little considered: the RPD was assumed to be uniform.

Recently, however, it was found that the reinjection mechanism is another important factor on the scaling property of the intermittency [5] and that various characteristic relations appear in type-I intermittency according to the RPD for a given local Poincaré map such as $-\ln\epsilon$ and $\epsilon^{-\nu}$ $(0 \leq \nu \leq 1/2)$. When the lower bounds of the reinjection (LBR) are below and above the tangent point the critical exponent is always $-1/2$ and 0, respectively, regardless of the RPD. But when the LBR is at the tangent point the characteristic relations have various critical exponents according to the RPD such that when the RPDs are uniform, fixed, and of the form $x^{-1/2}$, the characteristic relations are $-\ln\epsilon$, $\epsilon^{-1/2}$, and $\epsilon^{-1/4}$, respectively. The general form of the characteristic relations of type-I intermittency was also obtained for that of the local Poincaré map and the RPD by using renormalization group analysis [9]. The characteristic relations of type-II and -III intermittencies were also obtained according to the RPD [10]. But, there has been no experimental observation of the effect of the RPD on the scaling properties of intermittency. In this paper we report an experimental observation of the characteristic relations of type-I intermittency due to the RPD. We use the well-studied simple nonlinear electronic circuit, which is a series connected inductance L, resistance R, and junction diode, driven by an oscillator with bias voltage such as $V_0 \sin(2\pi\nu t) + V$.

II. EXPERIMENTAL SETUP

The electronic circuit can be easily set up in a laboratory and such features of the chaotic behavior have been studied as crisis [11], Feigenbaum's universality [12], noise effects [13], intermittency of which critical exponent is $-1/2$ [14], and Hopf bifurcations [15]. Effects from a system with a slow reverse recovery time diode have been analyzed many ways: by Hunt *et al.* on the basis of the effect of the reverse recovery time [16]; by Brorson *et al.* on the basis of total nonlinearity of the junction and diffusion capacitance [17]; by Kim *et al.* on the basis of the nonlinear junction capacitance in the case of fast recovery diode [18]. In the studies, the authors have varied the amplitude of the external oscillator by fixing the bias voltage to be 0. But the system also generates various chaotic phenomena as the bias voltage is varied when the amplitude and frequency of the external oscillator are fixed. In our experiment, therefore, the amplitude and frequency of the external oscillator are fixed at $V_0 = 5$ V and $\nu = 24$ kHz, respectively, and the bias voltage is varied for its easier controllability.

*Electronic address; chmkim@woonam.paichai.ac.kr

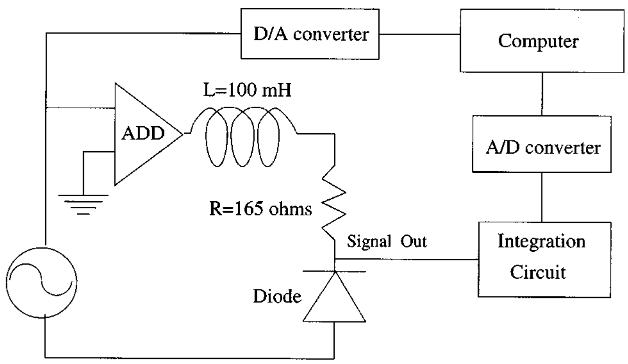

FIG. 1. Schematic diagram of experimental setup.

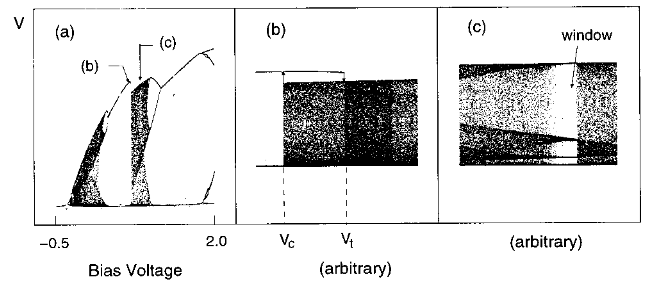

FIG. 2. The bifurcation diagram (a) from -0.75 V to 2.0 V, and enlarged diagram (b) around hysteresis crisis near period-3 window, and (c) near period-5 tangent bifurcation point.

In the experiment, a 100 mH inductor (165 Ω of dc resistance) and a DSDI12-16A silicon junction diode which has a heat sinker are connected to a function generator (Tektronix, FG 501A) in series. The bias voltage is varied by using the offset of the function generator and the voltage generated from a digital to analog (D-A) converter which is controlled by a personal computer. All the external forces are added by using operational amplifiers. We measure the rectified voltage across the diode and each rectified voltage pulse is integrated by using an integrating circuit to obtain experimental data. Through the experiment we guarantee that the peaks of the rectified pulses correspond to those of the integrated pulses. We add 0.6 V dc voltage to the rectified pulses before integration because the voltage drop of the silicon diode is -0.6 V when it is conducting. The peaks of integrated pulses are stored in the 40-Mbyte memory of the Pentium Computer by using expanded memory manager (EMM) through a 12-bit analog to digital (A-D) converter. All the systems are synchronized to one another. The digitized time of the A-D converter is 12 μsec. The digitized value of ± 2048 correspond to ± 5 V, respectively. In the integration of the rectified pulses, when V_0 is higher than 5 V, the highest integration pulses are distorted because the peak of the rectified pulse is higher than 15 V. So in the experiment we fix $V_0 = 5$ V. The chaotic outputs of the rectified and integrated pulses are also monitored by using a digital storage oscilloscope (LeCroy 9310). The noises from the power sources are reduced by using bypass capacitors. The schematic diagram of the experimental setup is given in Fig. 1.

III. RESULTS AND DISCUSSION

In this system, we observe various transitions from chaotic bands to stable fixed points as we vary the bias voltage V. Figure 2(a) is the bifurcation diagram obtained in the range of the bias voltage from about -0.75 V to about 2.0 V. In the figure, we can see a wide period-3 window in the range from about -0.01 V to about 0.63 V. At the end of the window, one of the stable fixed points does not collide with the chaotic band, which is the so-called hysteresis crisis [11]. And around 0.82 V we also observe a narrow period-5 window although it does not appear in this figure because of the resolution. In this window, one of the stable fixed points collides with the top end of the chaotic band [19]. What we are interested in here is the intermittency appearing in these windows since when the LBR is above the tangent point hysteresis crisis occurs, and when the LBR is at the tangent point, one of the stable fixed points collides with the chaotic band at the top or down end of the chaotic band. Figures 2(b) and 2(c), which show the windows clearly are the enlarged bifurcation diagrams around the bifurcation points of the period-3 and -5 window, respectively.

Hysteresis crisis appears clearly in Fig. 2(b). When the bias voltage increases, the stable fixed point suddenly jumps down to the chaotic band at the bifurcation point, $V=V_t$, and when it decreases, the chaotic band jumps up to the stable fixed point at the crisis point, $V=V_c$. In the region between the two points ($V_t>V_c$), there are two coexisting attractors, the stable and the chaotic. And Fig. 2(c) clearly shows that a stable orbit collides with the top end of the chaotic band. In the figure when the bias voltage decreases from the bifurcation point of the period-5 window, we can observe a chaotic bursts between quasiregular period-5 pulses. And when the bias voltage increases from the bifurcation point, we can observe a very narrow region of the period-5 window. When we increase the bias voltage more from the window, we can observe the transition from the periodic orbit to the chaotic band. To obtain the enlarged bifurcation diagram, we reduce the voltage from the D-A converter to be 1/50 using series connected resistors and roughly adjust the bifurcation point first controlling the offset of the function generator. In addition, we cannot find a hysteresis crisis around the period-5 window when we observe the bifurcation diagram by increasing and decreasing the bias voltage. This means the stable orbit collides with the chaotic band.

To show the intermittent behaviors of the system we have obtained the temporal behaviors of the system around period 3-tangent and period 5-tangent intermittencies. Figure 3(a) shows period 3-T intermittency at about $V=0.64$ V after crisis. It shows short laminar phases. When we decrease the bias voltage to about $V=0.62$ V the intermittency is abruptly changed to a stable 3-T period because of the hysteresis crisis. The shape is given in Fig. 3(b). The temporal behaviors of period-5 intermittency are also obtained. Figures 3(c) and 3(d) show short laminar phases at about $V=0.815$ V and longer laminar phases at about $V=0.82$ V, respectively. On this window we cannot find hysteresis crisis.

To obtain the return map, the bias voltage is fixed at the point of $V<V_t$ or $V>V_t$ near the bifurcation point where period-5 intermittency appears. Figures 4(a) and 4(b) are x_n vs x_{n+5} return maps before and after the tangent bifurcation, respectively. Figure 4(a) shows that the maximum point at

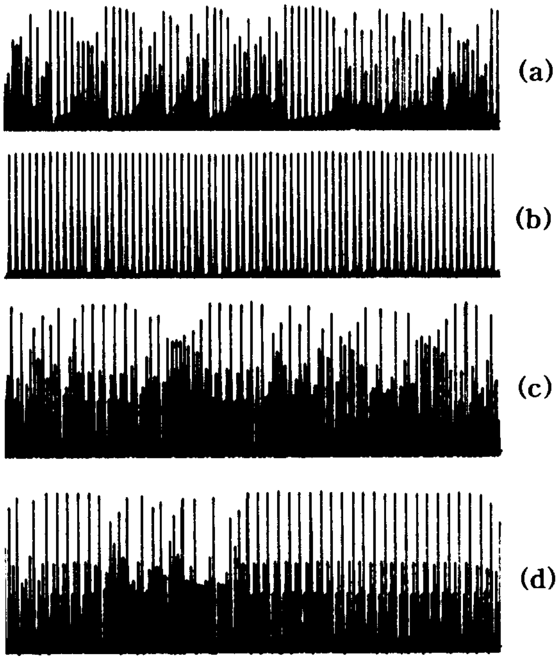

FIG. 3. Temporal behaviors of intermittency near hysteresis crisis on period-3 window and near period-5 window (a) after crisis and (b) before crisis on period-3 window and (c) short and (d) longer laminar phases of period-5 intermittency.

the right side of the return map is just below the diagonal. It means the LBR is very close to the tangent point. In the figure, the return map consists of two curves which merge at the maximum point of the right hump, and form a continuous curve. So the curve is imperfectly folded and it is double valued. This behavior also appears in x_n vs x_{n+1} as well as x_n vs x_{n+m} return maps for an arbitrary m. This phenomenon has already been observed in Refs. [10,13,20], and the authors have attributed it to the higher-dimensional property of the circuit. Although the map exhibits higher-dimensional property, we believe that the local Poincaré map of each

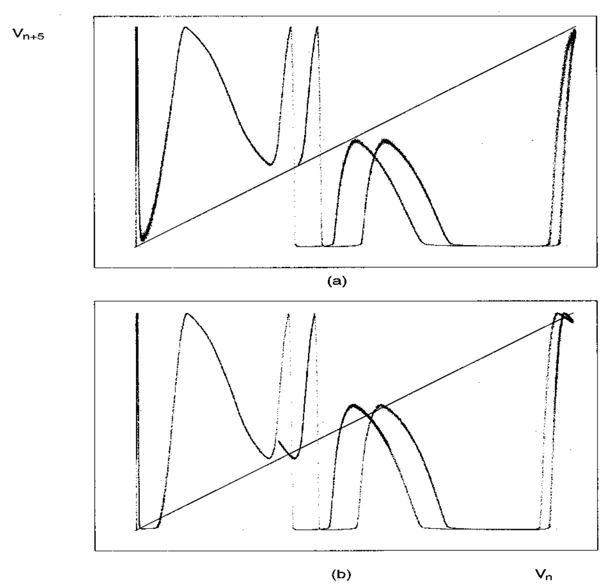

FIG. 4. The return map near period-5 window (a) before and (b) after the tangent bifurcation point.

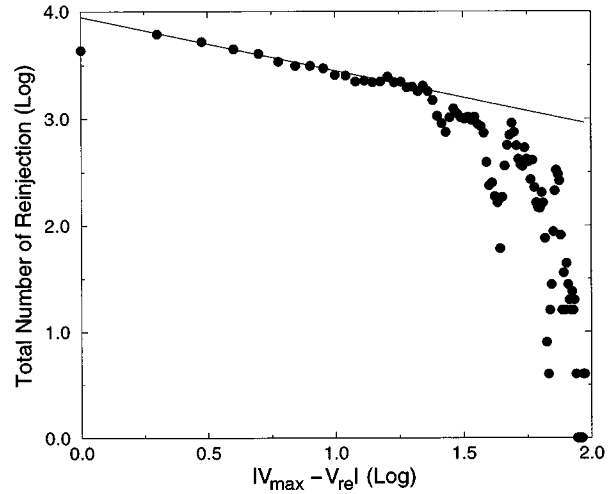

FIG. 5. RPD near period-5 window. The dots are experimental data and the solid line is the fitting of the data when $|V_{max}-V_{re}|$ is small. The slope of the solid line is $-1/2$ so the RPD is approximately of the form $x^{-1/2}$.

curve has the form of $x_{n+1}=ax_n^2+x_n+\epsilon$.

In the return map, although it is not clear that the local Poincaré map near the bifurcation point is of the form $x_{n+1}=x_n+a{x_n}^2+\epsilon$, it has been shown elsewhere that the bifurcation diagram is quite similar to the local Poincaré map of the logistic map, and that the first return map has a single quadratic maximum in the limit of sufficiently large resistance R. In accordance with these approximations, we consider that the local Poincaré map around the tangent point is quadratic. Figure 4(b) shows that the return map crosses over the diagonal line when the bias voltage is slightly higher than the bifurcation point. The two figures clearly show the characteristics of the return maps before and after the tangent bifurcation.

To obtain the RPD, we first measure the maximum digitized value of the chaotic band, $V_{max}=934$. And we let the lower gate be $V_c=830$. In the theoretical predictions, the gate size is not essential in obtaining characteristic relations. We count the total numbers of reinjections at each point, V_{re} in the gate. Figure 5 is a log-log plot of the total numbers of reinjections at each point vs $|V_{max}-V_{re}|$. As given in the figure, the slope of the RPD turns out to be about $-1/2$ if $|V_{max}-V_{re}|$ is small, which means that the reinjection probability distribution is of the form $1/\sqrt{x}$. In the figure, the $-1/2$ line matched the experimental data well within less than 1% of deviation and the form of the RPD is the same as that of Ref. [5]. To recapitulate, if the local Poincaré map around the tangent point is of the form $x_{n+1}=x_n+a{x_n}^2+\epsilon$ and the RPD is of the form $1/\sqrt{x}$, the characteristic relation is of the form $<l>\propto\epsilon^{-1/4}$. And in the case of the period-3 window, the characteristic relation is constant regardless of the RPD since the LBR is above the tangent point.

Figure 6 is a log-log plot of the average laminar phase lengths vs ϵ obtained at the period-3 (line B) and -5 windows (line A), where $\epsilon=|V_t-V|$. In the figure the dots are experimental results and the solid lines are obtained by fitting the dots when $|V-V_c|$ is less than 1 mV. The slopes of the solid lines are the critical exponents of the characteristic relations. In this measurement, we also reduce the bias voltage from

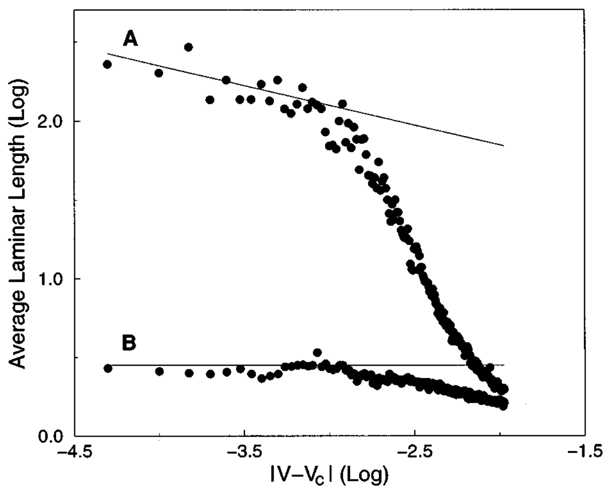

FIG. 6. The average laminar phase lengths vs $|V-V_t|$. The figure shows well that the critical exponents are $-1/4$, and 0, when the LBRs are at (line A) and above (line B) the tangent point, respectively. The dots are experimental data and the solid lines are the fitting of the data with the slope of $-1/4$ and 0, respectively, when $|V-V_t|$ is small.

the D-A converter to be 1/50 for a fine tuning of ϵ after adjusting the offset of the function generator near to the bifurcation point in the window. The step size of the bias voltage from the D-A converter is about 0.05 mV. As the bias voltage reduces the length of the longest laminar phase is counted and if the length of the longest laminar phase is less than 10^4, the data begin to be stored in the computer. We assume that the last point where the length of the longest laminar phase is larger than 10^4 is the bifurcation point. In the experiment, if the length of the longest laminar phase is larger than 10^4, we cannot observe the chaotic bursts between regular periods. And at each bias voltage, 10^4 laminar phases are obtained and 220 steps of total step size are varied which correspond to about 11 mV of total variation. We note here, if $1 \gg \epsilon > |x_{\mathrm{LBR}} - x_t|$ where x_{LBR} is the lower bound of the reinjection point, we can obtain $-1/4$ of critical exponent.

In the figure, line A shows well that the characteristic relation is of the form $\langle l \rangle \propto |V-V_t|^{-\nu}$ with approximately $\nu \approx 0.25$ when $|V-V_t|$ is small enough. The error deviation of line A is less than 7%. The figure also shows a rapid decay of the average laminar phase lengths when $|V-V_t|$ is large. The critical exponent, where $|V-V_t|$ is small, is $-1/4$ the same one previously obtained theoretically when the LBR is at the tangent point. And the average laminar phase lengths of line B are constant when $|V-V_t|$ is small. The results again agree well with the theoretical predictions when LBR is above the tangent point. The two lines clearly show the characteristic relations due to the RPD in the experiment.

IV. CONCLUSION

In summary, the inductance-resistance-diode circuit shows not only hysteresis crisis when the LBR is above the tangent point but also that the stable periodic orbit collides with the top end of the chaotic band when the LBR is at the tangent point. In these regions where intermittency appears, the RPD is of the form $x^{-1/2}$. So two critical exponents appear, $-1/4$ and 0, when the LBRs are at and above the tangent point, respectively. The results experimentally verify the characteristic relations of type-I intermittency due to the RPD.

ACKNOWLEDGMENT

This study was supported by Nondirected Research Fund, Korea Research Foundation.

[1] C. Grebogi, E. Ott, and J. A. Yorke, Phys. Rev. Lett. **50**, 93 (1983); W. L. Ditto *et al.*, *ibid.* **63**, 923 (1989); J. C. Sommerer, W. L. Ditto, C. Grebogi, E. Ott, and M. L. Spano, *ibid.* **66**, 1947 (1991).

[2] N. Platt, E. A. Spiegel, and C. Tresser, Phys. Rev. Lett. **70**, 279 (1993); P. W. Hammer, N. Platt, S. M. Hammel, J. F. Heagy, and B. D. Lee, *ibid.* **73**, 1095 (1994).

[3] Y. Pomeau and P. Manneville, Commun. Math. Phys. **74**, 189 (1980); H. Kaplan, Phys. Rev. Lett. **68**, 553 (1992); J. E. Hirsch, P. Manneville, and J. Scalapino, Phys. Rev. A **25**, 519 (1982); B. Hu and J. Rudnick, Phys. Rev. Lett. **48**, 1645 (1982); P. Berg, M. Dubois, P. Manneville, and Y. Pomeau, J. Phys. (France) Lett. **41**, L344 (1980); J.-Y. Huang and J.-J. Kim, Phys. Rev. A **36**, 1495 (1987); M. Dubois, M. A. Rubio, and P. Berg, Phys. Rev. Lett. **51**, 1446 (1983).

[4] H. G. Schuster, *Deterministic Chaos*, 2nd revised ed. (VCH Publishers, Weinheim, 1987).

[5] C.-M. Kim, O. J. Kwon, E. K. Lee, and H. Lee, Phys. Rev. Lett. **73**, 525 (1994).

[6] M. Bauer, S. Habip, D. R. He, and W. Martienssen, Phys. Rev. Lett. **68**, 1625 (1992).

[7] B. Hu and J. Rudnick, Phys. Rev. A **26**, 3035 (1982); A. B. Zisook, *ibid.* **25**, 2289 (1982).

[8] The typical Poincaré map of type-II intermittency is composed of $\theta_{n+1} = \theta_n + \Omega$ as well as $y_n + 1 = (1+\epsilon) y_n + a y_n^3$. However, the radius variation alone can determine the average laminar length and consequently the characteristic relation.

[9] O. J. Kwon, C.-M. Kim, E. K. Lee, and H. Lee, Phys. Rev. E **53**, 1253 (1996).

[10] M. O. Kim, H. Lee, C.-M. Kim, E. K. Lee, and O. J. Kwon, Int. J. Bifurcation Chaos Appl. Sci. Eng. (to be published).

[11] C. Jeffries and J. Perez, Phys. Rev. A **27**, 601 (1983); H. Ikezi, J. S. deGrassie, and T. H. Jensen, *ibid.* **28**, 1207 (1983).

[12] J. Testa, J. Perez, and C. Jeffries, Phys. Rev. Lett. **48**, 714 (1982).

[13] J. Perez and C. Jeffries, Phys. Rev. B **26**, 3460 (1982).

[14] C. Jeffries and J. Perez, Phys. Rev. A **26**, 2117 (1982).

[15] R. V. Buskirk and C. Jeffries, Phys. Rev. A **31**, 3332 (1985).

[16] E. R. Hunt, Phys. Rev. Lett. **49**, 1054 (1982); R. W. Rollins and E. R. Hunt, *ibid.* **49**, 1295 (1982).

[17] S. T. Brorson, D. Dewey, and P. S. Linsay, Phys. Rev. A **28**, 1201 (1983).

[18] C.-M. Kim, C. H. Cho, C. S. Lee, J. H. Yim, J. Kim, and Y. Kim, Phys. Rev. A **38**, 1545 (1988).

[19] When the flow drection is positive, hysteresis crisis occurs if LBR is above the tangent point, and when flow direction is negative, it occurs if the upper bound of the reinjection is below the tangent point. While in theoretical interpretation general flow direction is positive, in our experiment, the flow direction is negative. But here, we will discuss the system dynamics as positive flow direction without loss of generality.

[20] E. R. Hunt and R. W. Rollins, Phys. Rev. A **29**, 1000 (1984).